Electromagnetic Dissociation and Spacecraft Electronics Damage

John W. Norbury
NASA Langley Research Center
Hampton, VA 23681, USA
757-864-1480
john.w.norbury@nasa.gov

***Abstract*—When protons or heavy ions from galactic cosmic rays (GCR) or solar particle events (SPE) interact with target nuclei in spacecraft, there can be two different types of interactions. The more familiar strong nuclear interaction often dominates and is responsible for nuclear fragmentation in either the GCR or SPE projectile nucleus or the spacecraft target nucleus. (Of course, the proton does not break up, except possibly to produce pions or other hadrons.) The less familiar, second type of interaction is due to the very strong electromagnetic fields that exist when two charged nuclei pass very close to each other. This process is called electromagnetic dissociation (EMD) and primarily results in the emission of neutrons, protons and light ions (isotopes of hydrogen and helium). The cross section for particle production is approximately defined as the number of particles produced in nucleus-nucleus collisions or other types of reactions. (There are various kinematic and other factors which multiply the particle number to arrive at the cross section.) Strong, nuclear interactions usually dominate the nuclear reactions of most interest that occur between GCR and target nuclei. However, for heavy nuclei (near Fe and beyond) at high energy the EMD cross section can be much larger than the strong nuclear interaction cross section. This paper poses a question: Are there projectile or target nuclei combinations in the interaction of GCR or SPE where the EMD reaction cross section plays a dominant role? If the answer is affirmative, then EMD mechanisms should be an integral part of codes that are used to predict damage to spacecraft electronics. The question can become more fine-tuned and one can ask about total reaction cross sections as compared to double differential cross sections. These issues will be addressed in the present paper.**

TABLE OF CONTENTS

1. INTRODUCTION

Galactic cosmic rays (GCR) and solar particle events (SPE) are known to be significant radiation hazards in space for both humans and electronic components [1], [2], [3], [4]. GCR contain all nuclei in the periodic table with energies extending to hundreds of GeV/nucleon (n) and beyond [5]. SPE contain mainly protons, with some heavier ions such as helium being present also. SPE nuclear energies are often in the hundreds of MeV/n region and are usually less than 1 GeV/n [5].

978-1-4673-7676-1/16/$31.00

The present paper will focus mainly on GCR interactions, whereby nuclei present in the external field are broken up into lighter fragments upon collision with target nuclei. The target nuclei represent nuclei making up spacecraft shielding, or nuclei present in the human body, or nuclei present in electronic components, etc. These reactions are called nucleus - nucleus collisions and can result in reaction products different from the projectile or target nuclei. For example, one reaction might be ^{56}Fe + Al $\rightarrow$ ^{55}Fe + n + Al, which represents an ^{56}Fe nucleus in the GCR field interacting with an Al nucleus in the spacecraft shielding, with the ^{56}Fe nucleus breaking up into a neutron (n) and a lighter isotope ^{55}Fe. Nuclear reactions are quantified by calculating a cross section, which represents the probability of a particular reaction occurring. These nuclear reaction cross sections are fundamental inputs into space radiation transport codes. In the following, the spectrum represents the abundance (number of nuclei) versus energy for a given nucleus. Given the full external GCR spectrum for each nucleus present in the GCR, which is incident on the outside spacecraft wall, and given the full set of nuclear reaction cross sections, a space radiation transport code can then be used to calculate the spectrum of nuclear particles produced inside the spacecraft. This secondary spectrum can then be used to predict various forms of damage to humans or electronic components.

The four known forces of nature are the strong, weak, electromagnetic (EM) and gravitational interactions, mediated by pions (or gluons), vector bosons, photons and gravitons respectively. All of these mediating particles are "virtual", with properties different from "real" particles. Gravitational interactions are negligible for GCR reactions, and weak interactions are only relevant for the decay of produced particles, such as muon decay, and are not relevant for the GCR nucleus - nucleus reactions referred to above. Space radiation transport codes therefore often only include strong interaction processes when cross section calculations are made and used as input for radiation transport. The question to be addressed in the present work concerns the importance of electromagnetic interactions when calculating reaction cross sections.

The range of strong interactions is about one fermi (fm = 10^{-15} m), and so they are important only if the projectile and target nuclei physically overlap during the reaction. This is shown in Figure 1, which is a pictorial representation of the ^{56}Fe + Al $\rightarrow$ ^{55}Fe + n + Al reaction, showing the nuclei overlapping and undergoing a strong interaction, causing a neutron to be emitted from the projectile nucleus. Such strong interaction reactions occur either with direct production of the neutron or other produced particle (via knockout, stripping,

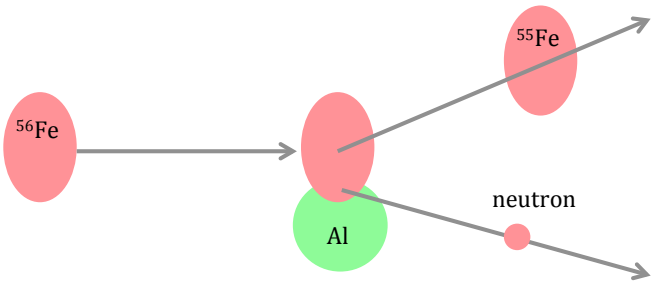

Figure 1. Strong nuclear reaction seen from the rest frame of the target nucleus. The reaction ^{56}Fe + Al $\rightarrow$ ^{55}Fe + n + Al is mediated by the short range strong interaction when the projectile and target nuclei overlap. The oval shape of the projectile nucleus is the relativistic Lorentz contraction as seen from the target rest frame.

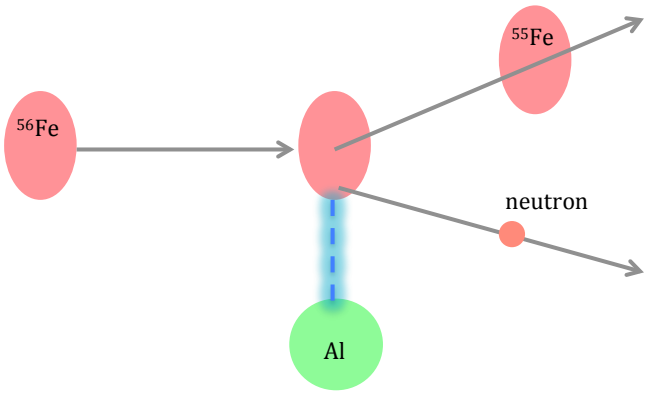

Figure 2. The reaction ^{56}Fe + Al $\rightarrow$ ^{55}Fe + n + Al is mediated by the long range EM interaction when the projectile and target nuclei miss each other and do not overlap. The blue dashed line represents a virtual photon being exchanged, resulting in a very large electric field between the two nuclei, causing one of them to break up.

pickup etc.), or through an intermediate mechanism, known as abrasion - ablation, whereby a piece of the projectile is sheared off (abrasion) and left in a highly excited state which can then decay (ablation) resulting in the production of a variety of particles including neutrons.

EM interactions have a very long (infinite) range. The distance of closest approach between the projectile and target is random. When the projectile and target nuclei miss each other and do not overlap (typically at distances larger than several fm) the strong interactions are not effective and the EM interactions are dominant. Even though several fm is a "large" distance, so that strong interactions are not effective, it is still an extremely short distance on macroscopic scales. One is bringing two highly charged nuclei to a distance of several fm and so the electric field between the nuclei will be extremely large. (In fact, it can be so large as to cause the vacuum to break down and decay into electron - positron pairs, in a manner analogous to dielectric breakdown with strong electric fields. This is not the topic of the present work, but is discussed in [6]). The EM reaction process is shown in Figure 2, where the interaction is mediated by the exchange of a virtual photon. Figures 1 and 2 show the same reaction ^{56}Fe + Al $\rightarrow$ ^{55}Fe + n + Al being mediated by the different strong and EM interactions. Whereas the strong interaction process can cause the neutron to be knocked out either directly or via an intermediate excited projectile state, the EM interaction typically causes the projectile nucleus to start vibrating internally (called the giant dipole resonance), and subsequently de-exciting with the emission of a neutron, or other particles.

The discussion above has emphasized the breakup of the projectile nucleus, with the virtual photon being emitted by the target. Of course, the symmetric reaction will also occur, where the target breaks up and the virtual photon is emitted by the projectile.

2. Electromagnetic Dissociation

The breakup of a nucleus via EM interactions is called electromagnetic dissociation (EMD), and its importance for space radiation processes has been discussed extensively in the literature [7], [8]. However, the applications to spacecraft electronics damage, which is the topic of the present work, has not been addressed previously.

In the discussion below, it will be important to understand the different reference frames. Figures 1 and 2 show the reactions proceeding, as seen from the target rest frame (often called the "lab" frame). An observer in the target rest frame sees the projectile moving past at very high speed (energy) and observes the relativistic Lorentz contraction of the projectile nucleus, resulting in distortion into a "pancake" shape. One could also observe the reaction from the projectile rest frame, and one would see the Lorentz contracted target moving past at high speed. This latter viewpoint from the projectile frame, explains the source of high energy virtual photons that impinge on the projectile nucleus. From the projectile frame viewpoint, one sees a highly charged nucleus traveling past at high speed, resulting in high energy virtual photons emanating from the target nucleus. These photons impact the projectile, causing it to break up.

Figure 2 shows two aspects of the EMD reaction. The target nucleus (Al) is a source of virtual photons with a well defined spectrum $N(E_\gamma)$, where N is the number of virtual photons with energy E_γ. These virtual photons interact with the projectile nucleus resulting in a photon - nucleus interaction, often simply called a photonuclear interaction [9]. The EMD calculation will therefore involve calculating both the virtual photon spectrum $N(E_\gamma)$ and the photonuclear reaction cross section $\sigma(E_\gamma)$, which is also a function of the virtual photon energy E_γ. The full EMD cross section is then obtained by integrating these two quantities, as in [8]

$$\sigma_{\rm EMD} = \int dE_\gamma \, N(E_\gamma) \, \sigma(E_\gamma). \qquad (1)$$

The limits of integration are from 0 to ∞, but in practice the lower energy limit is the photonuclear energy threshold for producing a particular particle and the upper limit is the virtual photon spectrum "cut-off", calculated from a consideration of the distance of closest approach of the two nuclei (roughly the sum of the nuclear radii) [8] and the energy of the incoming projectile nucleus, which provide an effective upper energy limit to the photons. For the example EMD reaction, ^{56}Fe + Al $\rightarrow$ ^{55}Fe + n + Al, the relevant photonuclear cross section $\sigma(E_\gamma)$ is for the reaction γ + ^{56}Fe $\rightarrow$ ^{55}Fe + n, where the virtual photon γ comes from the Al target nucleus.

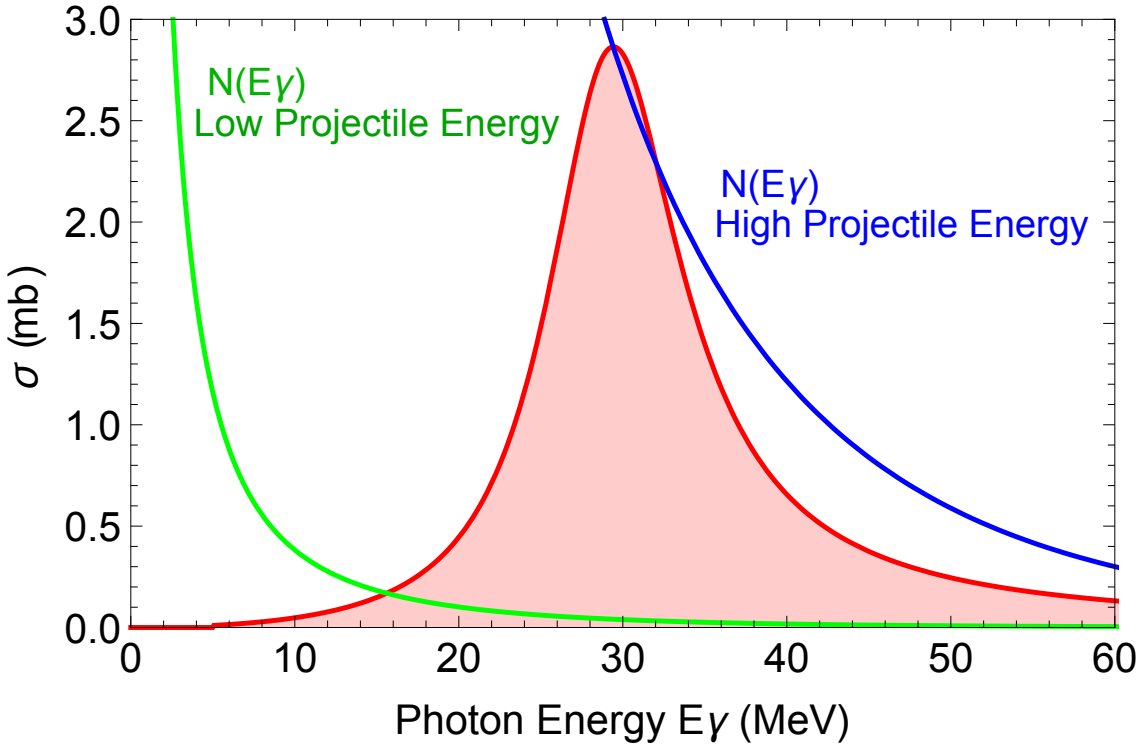

Figure 3. A typical photonuclear cross section $\sigma(E_\gamma)$ is shown by the red curve, plotted against photon energy E_γ on the horizontal axis. The green and blue curves show typical virtual photon spectra $N(E_\gamma)$ for low and high energy projectiles (or equivalently low and high energy targets as seen in the projectile frame). The label of vertical axis refers to the photonuclear cross section, in units of millibarn (mb). For the virtual photon spectrum, the vertical axis scale is not shown.

Methods for calculating $N(E_\gamma)$ and $\sigma(E_\gamma)$ are described extensively in reference [8], and will not be repeated here. However, some explanatory remarks will now be made. The integral in equation (1) involves the overlap of the virtual photon spectrum $N(E_\gamma)$ with the photonuclear cross section $\sigma(E_\gamma)$. A typical photonuclear cross section is shown in Figure 3 as the Lorentzian bell-shaped red curve, typical of the giant dipole resonance, whereby an incoming photon causes the entire nucleus to be excited into a large vibrational state. The central resonance energies are typically tens of MeV as seen in the Figure. Superimposed in Figure 3 are examples of the spectrum of virtual photons provided by the target. If one is stationary in the projectile frame, then one sees the charged target nucleus passing by at high speed, producing the virtual photon spectrum. The faster, or higher energy, that the projectile moves will correspond to a higher energy moving target, as seen in the projectile rest frame. One therefore expects that a high energy projectile will see a much larger flux of high energy virtual photons provided by the target. This is seen in Figure 3, where there are many more higher energy photons for the higher energy projectile. The overlap between $N(E_\gamma)$ and $\sigma(E_\gamma)$ is small for low energy projectiles, resulting in a small EMD cross section as calculated in equation (1). At high projectile energy, the overlap is large resulting in a large EMD cross section.

3. RESULTS

Cross section calculations for EMD and strong interactions are shown in Tables 1 and 2 for C and Fe projectiles respectively, for Al, Fe and Au targets. The projectile energies are 300 MeV/n and 1 and 10 GeV/n. Strong interaction cross sections are calculated according to the NUCFRG3 model [10]. The EMD cross sections however were not calculated with the NUCFRG3 model [10], but were rather calculated with the new model [8]. This latter point requires some explanation. Consider, for example, the inclusive reaction (those in which only one final product is specified),

$$^{12}\mathrm{C} + \mathrm{Al} \;\rightarrow\; ^{8}\mathrm{Be} + \mathrm{X} + \mathrm{Al}, \tag{2}$$

where X represents anything else. The notation is that the projectile ^{12}C is written first, followed by the target Al. Two exclusive reactions that contribute to reaction (2) are alpha (α) particle production

$$^{12}\mathrm{C} + \mathrm{Al} \;\rightarrow\; ^{8}\mathrm{Be} + \alpha + \mathrm{Al}, \tag{3}$$

and two proton (p) and two neutron (n) production

$$^{12}\mathrm{C} + \mathrm{Al} \;\rightarrow\; ^{8}\mathrm{Be} + 2\mathrm{p} + 2\mathrm{n} + \mathrm{Al}. \tag{4}$$

In order to calculate the cross section for ^{8}Be production, as in reaction (2), one should include both exclusive reactions (3) and (4). In the NUCFRG3 model, this is how the strong interaction cross sections are calculated [10]. However, the EMD model in NUCFRG3 [10] was only able to calculate production of proton (p), neutron (n) deuteron (d), triton(t), helion (h), alpha (α). Multiple nucleon production, such as 2p or 2n was not able to be calculated in the EMD model of NUCFRG3, even though it was able to be calculated for strong interactions. Thus, NUCFRG3 was not capable of including reaction (4). The model of reference [8] improved

the EMD calculations in general, and also the effects of multiple nucleon removal were included. Thus the EMD model in reference [8] is able to include both reactions (3) and (4) and is the reason for using it in the present work. In addition, reference [8] also improved the calculations of proton (p), neutron (n) deuteron (d), triton(t), helion (h), and alpha (α) clusters and provided much better agreement with experiment [8]. Thus, the present work uses the strong interaction cross sections from NUCFRG3 [10] and the EMD cross sections from reference [8]. The coalescence model of NUCFRG3 was turned off for simplicity. Coalescence effects can be included in a later work, but it is not expected to change the qualitative conclusions of the present work. Tables 1 and 2 give the strong and EMD cross sections for a variety of fragments produced. For most reactions the strong interaction cross section is much larger than the EMD cross section. For example, Table 1 shows that for the reaction

$$^{12}\mathrm{C} + \mathrm{Al} \rightarrow {}^{11}\mathrm{C} + \mathrm{X} + \mathrm{Al} \quad (5)$$

at 1 GeV/n, the strong cross section is 66 millibarn (mb), while the EMD cross section is only 1 mb.

However, for some reactions, the EMD cross section is comparable to the strong cross section. For example, Table 2 shows that for the reaction

$$^{56}\mathrm{Fe} + \mathrm{Fe} \rightarrow {}^{55}\mathrm{Mn} + \mathrm{X} + \mathrm{Fe} \quad (6)$$

at 10 GeV/n, the strong cross section is 69 mb, while the EMD cross section is 77 mb. When the EMD cross section is more than half of the strong cross section, as this example shows, the EMD cross sections are listed in blue color in Tables 1 and 2.

Occasionally, the EMD cross section is much larger than the strong cross section. For example, Table 2 shows that for the reaction

$$^{56}\mathrm{Fe} + \mathrm{Au} \rightarrow {}^{55}\mathrm{Fe} + \mathrm{X} + \mathrm{Au} \quad (7)$$

at 10 GeV/n, the strong cross section is only 83 mb, compared to the very large EMD cross section of 1574 mb. When the EMD cross section is more than double the strong cross section, as this example shows, the EMD cross sections are listed in red color in Tables 1 and 2. These red colored cross sections are seen to occur much more often for heavy targets, especially Au, and usually involve the highest LET projectile fragments. Therefore, one can conclude that EMD reaction cross sections in projectile nuclei are much larger than strong reaction cross sections when the projectiles collide with heavy target nuclei.

One can also consider EMD reactions in the target nuclei, with the projectile now being the source of virtual photons. Table 3 shows calculations for C and Fe projectiles with EMD occurring in ^{197}Au targets. Similar to above, one can conclude that EMD reaction cross sections in target nuclei are much larger than strong reaction cross sections when the projectiles collide with heavy targets. Again it can be seen that EMD interaction cross sections are much larger than the strong interaction cross sections for the highest linear energy transfer (LET) target fragments, such as ^{196}Au and ^{195}Au.

The typical construction material used in spacecraft is aluminum (Al). The projectiles carbon (C) and iron (Fe) are typical projectiles in the galactic cosmic ray spectrum. It can be seen that for Al targets the EMD cross sections are rarely important and if left out of a space radiation transport code, the EMD effects are not likely to be noticed. This is also true if the dominant material in an electronic component is silicon (Si). However, sometimes heavier materials are present in electronic components. An example is gold (Au). In that case the EMD cross sections can be much larger than the strong cross sections. It is interesting to note that the reactions with the largest EMD cross sections are precisely those that produce the highest LET fragments. For the example of ^{56}Fe + Au, Table 2 shows that the EMD cross sections are largest for the reactions which produce ^{55}Fe, ^{55}Mn, ^{54}Fe, ^{54}Cr fragments. Such high LET fragments are known to be among those that produce the most damage in spacecraft electronic components [1].

In the above example, the corresponding exclusive reactions are

$$^{56}\mathrm{Fe} + \mathrm{Au} \rightarrow {}^{55}\mathrm{Fe} + \mathrm{n} + \mathrm{Au} \quad (8)$$
$$\rightarrow {}^{55}\mathrm{Mn} + \mathrm{p} + \mathrm{Au} \quad (9)$$
$$\rightarrow {}^{54}\mathrm{Fe} + \mathrm{n} + \mathrm{n} + \mathrm{Au} \quad (10)$$
$$\rightarrow {}^{54}\mathrm{Cr} + \mathrm{p} + \mathrm{p} + \mathrm{Au} \quad (11)$$

representing single neutron, single proton, double neutron and double proton removal respectively. The EMD reactions are not only copious sources of the highest LET fragments, but they are also significant sources of neutrons and protons, which are also of concern for spacecraft electronics [1]. Similarly, for the target reactions

$$\mathrm{Fe} + {}^{197}\mathrm{Au} \rightarrow \mathrm{Fe} + {}^{196}\mathrm{Au} + \mathrm{n} \quad (12)$$
$$\rightarrow \mathrm{Fe} + {}^{195}\mathrm{Au} + \mathrm{n} + \mathrm{n} \quad (13)$$

which also show copious production of neutrons due to the large EMD cross sections.

4. CONCLUSIONS

The present work has shown that EMD processes dominate the nuclear reaction mechanisms for the production of high LET fragments when heavy materials are present in spacecraft or electronic components. Therefore, in order to properly predict single event effects and other upset processes it is important to make sure that EMD processes are included in the nuclear reaction components of space radiation transport codes, especially if significant quantities of heavy elements are present in spacecraft or electronic components. These results also imply that if one needs to include heavy projectiles, such as lead (Pb), in the GCR spectrum then the corresponding EMD cross sections will also be very large.

5. SUMMARY

High energy nucleus - nucleus collisions occur when galactic cosmic ray projectile nuclei strike target nuclei in spacecraft, tissue materials, electronic components, etc. The dominant reaction mechanism is usually due to strong interactions whereby particles are produced either through abrasion - ablation or direct production. Electromagnetic dissociation is the process whereby a photon from the target nucleus excites the projectile (or vice-versa), which subsequently decays with the emission of heavy fragments and lighter particles. For medium mass target nuclei, the strong interaction reaction occurring in projectiles or targets typically dominate EMD processes. However, for heavy targets, such as Au that occur

Table 1. Calculated cross sections (mb) for C projectile nuclei undergoing strong and EMD interactions. Numbers in blue or red represent EMD cross sections bigger than half or bigger than double the strong interaction cross section.

Projectile		$^{12}C_6$								
Target		Al			Fe			Au		
Projectile Energy (GeV/n)		0.3	1	10	0.3	1	10	0.3	1	10
Fragment	Interaction									
$^{11}C_6$	Strong	70	66	62	78	74	69	97	93	88
	EMD	1	1	4	2	4	14	9	25	**109**
$^{11}B_5$	Strong	70	66	62	78	74	69	97	93	88
	EMD	2	2	6	4	7	23	17	42	**178**
$^{10}C_6$	Strong	1	1	1	1	1	1	1	1	1
	EMD	0	0	1	0	1	2	1	2	**16**
$^{10}Be_4$	Strong	5	5	5	6	6	6	8	7	7
	EMD	0	1	2	1	2	**8**	4	**13**	**65**
$^{10}B_5$	Strong	88	84	82	99	95	92	124	120	118
	EMD	0	0	1	0	1	2	1	2	17
$^{9}B_5$	Strong	7	7	7	8	8	8	10	10	10
	EMD	0	0	0	0	0	1	0	1	**8**
$^{9}Be_4$	Strong	31	30	28	35	33	32	44	43	41
	EMD	0	0	0	0	0	1	0	1	5
$^{8}Be_4$	Strong	7	6	6	7	7	7	9	9	9
	EMD	0	0	0	0	0	1	1	2	**11**

Table 2. Calculated cross sections (mb) for Fe projectile nuclei undergoing strong and EMD interactions. Numbers in blue or red represent EMD cross sections bigger than half or bigger than double the strong interaction cross section.

Projectile		$^{56}Fe_{26}$								
Target		Al			Fe			Au		
Projectile Energy (GeV/n)		0.3	1	10	0.3	1	10	0.3	1	10
Fragment	Interaction									
$^{55}Fe_{26}$	Strong	70	67	63	77	74	69	90	87	83
	EMD	13	19	**51**	**38**	**65**	**192**	**188**	**424**	**1574**
$^{55}Mn_{25}$	Strong	70	67	63	77	74	69	90	87	83
	EMD	5	8	20	16	27	**77**	**81**	**175**	**632**
$^{54}Fe_{26}$	Strong	71	68	65	18	17	17	21	21	20
	EMD	0	1	3	1	3	**12**	5	**17**	**97**
$^{54}Cr_{24}$	Strong	7	7	7	8	8	8	10	9	9
	EMD	1	2	**4**	3	**5**	2	**13**	**32**	**127**
$^{54}Mn_{25}$	Strong	71	68	65	79	76	75	94	91	89
	EMD	1	1	3	1	3	1	5	18	**93**
$^{53}Mn_{25}$	Strong	51	49	47	57	55	53	68	66	64
	EMD	0	0	1	1	1	2	1	3	22
$^{53}Cr_{24}$	Strong	23	22	21	26	25	24	31	30	29
	EMD	0	0	0	0	0	1	0	1	6
$^{52}Cr_{24}$	Strong	47	46	44	53	51	50	63	62	61
	EMD	0	0	1	0	1	4	5	10	**35**

Table 3. Calculated cross sections (mb) for Au target nuclei undergoing strong and EMD interactions. Numbers in blue or red represent EMD cross sections bigger than half or bigger than double the strong interaction cross section.

Target		$^{197}Au_{79}$					
Projectile		C			Fe		
Projectile Energy GeV/n		0.3	1	10	0.3	1	10
Fragment	Interaction						
$^{196}Au_{79}$	Strong	71	66	62	77	74	69
	EMD	21	29	**71**	**272**	**434**	**1226**
$^{196}Pt_{78}$	Strong	71	66	62	77	74	69
	EMD	0	0	0	2	2	7
$^{195}Au_{79}$	Strong	11	11	10	12	12	12
	EMD	3	**5**	**13**	**34**	**66**	**219**

sometimes in electronic components, the EMD processes are often much larger than strong interaction cross sections, especially for high LET fragments. Some examples were shown where the EMD cross sections are larger than 1000 mb! Therefore, space radiation transport codes that simulate radiation effects in electronic components, need to include EMD processes if significant quantities of heavy elements are present as either targets or projectiles.

ACKNOWLEDGMENTS

This work was supported by the Human Research Program under the Human Exploration and Operations Mission Directorate of NASA. I am very grateful to Drs. Lembit Sihver, Steve Blattnig, Tony Slaba, Francis Badavi, Steve Smith and Jonathan Ransom for reviewing the paper. I also thank Dr. Ryan Norman for help with the NUCFRG3 code and Drs. Anne Adamczyk, Charles Werneth, Lawrence Townsend and Khin Maung for many useful discussions.

REFERENCES

[1] C. Leroy, P.G. Rancoita, "Particle interaction and displacement damage in silicon devices operated in radiation environments," *Rep. Prog. Phys.*, vol. 70, pp. 493-625, 2007.

[2] F.W. Sextion, "Destructive single event effects in semiconductor devices and ICs," *IEEE Trans. Nuc. Sci.*, vol. 50, pp. 603-621, 2003.

[3] R.A. Reed, J. Kinnison, J.C. Pickel, S. Buchner, P.W. Marhall, S. Kniffin, K.A. LaBel, "Single event effects ground testing and on-orbit rate prediction methods: The past, present, and future," *IEEE Trans. Nuc. Sci.*, vol. 50, pp. 622-634, 2003.

[4] P.E. Dodd, L.W. Massengill, "Basic mechanisms and modeling of single event upset in digital microelectronics," *IEEE Trans. Nuc. Sci.*, vol. 50, pp. 583-602, 2003.

[5] M. Durante, F. Cucinotta, "Physical basis of radiation protection in space travel," *Rev. Mod. Phys.*, vol. 83, pp. 1245-1281, 2011.

[6] J.W. Norbury, "Pair production from nuclear collisions and cosmic ray transport," *J. Phys. G*, vol. 32, pp. B31-B35, 2006.

[7] J.W. Norbury, K.M. Maung, "Electromagnetic dissociation and space radiation," *Acta Astronautica*, vol. 60, pp. 770-774, 2007.

[8] J.W. Norbury, "Light ion and multiple nucleon removal due to electromagnetic dissociation," *Nucl. Instr. Meth. Phys. Res. A*, vol. 703, pp. 220-243, 2013.

[9] A.M. Adamczyk, J.W. Norbury, L.W. Townsend, "Weisskopf-Ewing and Hauser-Feshbach calculations of photonuclear cross sections used for electromagnetic dissociation," *Rad. Phys. Chem.*, vol. 90, pp. 21-25, 2013.

[10] A.M. Adamczyk, R.B. Norman, S.I. Sriprisan, L.W. Townsend, J.W. Norbury, S.R. Blattnig, T.C. Slaba, "NUCFRG3: Light ion improvements to the nuclear fragmentation model," *Nucl. Instr. Meth. Phys. Res. A*, vol. 678, pp. 21-32, 2012.

BIOGRAPHY

John W. Norbury *is leader of the Space Radiation Group at NASA Langley Research Center. He holds Bachelor and Master degrees in experimental nuclear physics from the University of Melbourne (Australia) and a Ph.D. in theoretical nuclear physics from the University of Idaho (USA). He has held positions as Professor of Physics and Physics Department Chair at the University of Wisconsin-La Crosse, the University of Wisconsin-Milwaukee and Worcester Polytechnic Institute. In 2004, he received the Distinguished Undergraduate Teaching Award from the University of Wisconsin-Milwaukee. From 1998 - 2000, Dr. Norbury was Director of the NASA Wisconsin Space Grant Consortium. He has published approximately 100 papers in externally refereed journals and has supervised seven doctoral dissertations. He was Scientific Director of the NASA Space Radiation Summer Schools in 2014 and 2015. Dr. Norbury is a Fellow of the Institute of Physics.*